ACS APPLIED NANO MATERIALS

UF University of Florida Libraries

Subscriber access provided by University of Florida | Smathers Libraries

Article

Enhanced piezocapacitive effect in CaCu3Ti4O12-polydimethylsiloxane composited sponge for ultrasensitive flexible capacitive sensor

chunhong Mu, Junpeng Li, Yuanqiang Song, Wutong Huang, Ao Ran, Kai Deng, Jian Huang, weihua xie, Rujie Sun, and Huaiwu Zhang

ACS Appl. Nano Mater., **Just Accepted Manuscript** • DOI: 10.1021/acsanm.7b00144 • Publication Date (Web): 21 Dec 2017

Downloaded from http://pubs.acs.org on December 23, 2017

Just Accepted

"Just Accepted" manuscripts have been peer-reviewed and accepted for publication. They are posted online prior to technical editing, formatting for publication and author proofing. The American Chemical Society provides "Just Accepted" as a free service to the research community to expedite the dissemination of scientific material as soon as possible after acceptance. "Just Accepted" manuscripts appear in full in PDF format accompanied by an HTML abstract. "Just Accepted" manuscripts have been fully peer reviewed, but should not be considered the official version of record. They are accessible to all readers and citable by the Digital Object Identifier (DOI®). "Just Accepted" is an optional service offered to authors. Therefore, the "Just Accepted" Web site may not include all articles that will be published in the journal. After a manuscript is technically edited and formatted, it will be removed from the "Just Accepted" Web site and published as an ASAP article. Note that technical editing may introduce minor changes to the manuscript text and/or graphics which could affect content, and all legal disclaimers and ethical guidelines that apply to the journal pertain. ACS cannot be held responsible for errors or consequences arising from the use of information contained in these "Just Accepted" manuscripts.

ACS Publications

ACS Applied Nano Materials is published by the American Chemical Society. 1155 Sixteenth Street N.W., Washington, DC 20036

Published by American Chemical Society. Copyright © American Chemical Society. However, no copyright claim is made to original U.S. Government works, or works produced by employees of any Commonwealth realm Crown government in the course of their duties.

Enhanced Piezocapacitive Effect in $CaCu_3Ti_4O_{12}$-Polydimethylsiloxane Composited Sponge for Ultrasensitive Flexible Capacitive Sensor

Chunhong Mu,[†] Junpeng Li,[†] Yuanqiang Song,[†] Wutong Huang,[†] Ao Ran,[†] Kai Deng,[†] Jian Huang,[‡] Weihua Xie,[*‡] Rujie Sun,[§] Huaiwu Zhang[*†]*

[†]State Key Laboratory of Electronic Thin Films and Integrated Devices, University of Electronic Science and Technology of China, No. 4 Section 2 Noth Jianshe road, 610054, PR China. E-mail: yuanqiangsong@uestc.edu.cn; hwzhang@uestc.edu.cn

[‡]Center for Composite Materials and Structures, No. 2 Yikuang Street, Nangang District, Harbin Institute of Technology (HIT), P.O. Box 301, Harbin 150080, PR China. Email: michael@hit.edu.cn

[§]ACCIS, University of Bristol, Queen's Building, University Walk, Bristol, BS8 1TR, United Kingdom.

KEYWORDS: Flexible pizeocapacitive sensor, high sensitivity, $CaCu_3Ti_4O_{12}$ nanoparticles, giant dielectric constant, inorganic-organic hybridization

ABSTRACT: Highly sensitive flexible piezocapacitive (PC) pressure sensor demonstrates wide applications in wearable electronics. In this paper, we first theoretically proposed an effective

strategy to improve the sensitivity of the PC pressure sensor, by constructing a porous dielectric layer composted of inorganics with high-dielectric constant (ε_H) and organics with low-dielectric constant (ε_L). By using $CaCu_3Ti_4O_{12}$ (CCTO) nanocrystals with giant ε as the dopant and polydimethylsiloxane (PDMS) with a low ε as the matrix, an ultra-soft CCTO-PDMS dielectric sponge was fabricated, *via* a simple porogen assisted process. The CCTO-PDMS composited sponge exhibits an ultra-low compression modulus of 6.3 kPa, a highly enhanced sensitivity with the gauge factor of up to 1.66 kPa^{-1} in a range of 0-640 Pa, and a response time of 33 ms, and that the sensitivity outperforms that of a pure PDMS and other PC sensors reported recently. This sensitivity enhancement is attributed to the hybridization of two phases of $\varepsilon_H/\varepsilon_L$ in the composites, which provides an effective route to other novel flexible PC sensors. In practical applications, CCTO-PDMS based PC sensor demonstrates potential applications, such as recording wrist pulse wave with fine accurate and fidelity, bending and twisting detection, Moss code simulating. The low-cost fabrication process in conjunction with its superior sensitivity, robustness of the functional versatility and mechanical flexibility make the CCTO-PDMS based pressure sensor wide promising applications in wearable devices, flexible electronics, robotics, etc.

1. INTRODUCTION

Pressure sensors with flexible and wearable characteristics have shown great potential applications in intelligent terminals such as health care monitoring/diagnosis devices,[1,2] smart robotics,[3,4] and energy harvesting.[5-7] Several pressure monitoring techniques have been explored based on different concepts including piezoelectric (PE),[8] piezoresistive (PR),[9] or piezocapacitive (PC)[10,11] effects, etc. From the view of applications, PC-type sensor has many

superiorities such as ultra-fast response, lower power consumption and smaller signal drift by temperature effects, making it more favorable especially for low-power touch-sensitive platforms and wireless applications in wearable smart components.[12]

PC-type pressure sensor is in fact a flexible capacitor, of which the capacitance is changed by the deformation of the sandwiched flexible dielectric layer. Normally, the sensitivity of a PC sensor is dependent on the flexibility and the microstructure of the sandwiched soft dielectric layer. To improve the sensitivity of the PC sensors, recent efforts have focused on modifying the mechanical properties by using microstructured dielectric materials. For PC sensors, microstructured polymer such as commercial polymer foams exhibit larger capacitance change and thus a higher sensitivity, than that of an unstructured dielectric material at an identical pressure level.[10,13,14]

A group of polymer matrix including polyurethane (PU) foams,[15,16] natural rubber,[17] poly (vinylidene fluoride) (PVDF),[18] and polydimethylsiloxane (PDMS),[19] have been intensively investigated for pressure monitoring applications. Among these flexible materials, PDMS is thought to be much more suitable for the PC sensors,[10,20] due to its high elasticity, excellent stretchability, as well as the high-temperature stability, low material costs, and non-toxicity.[21] PDMS-based elastomer has been intensively investigated aiming to explore flexible smart components for wearable electronics applications.[22-29] In order to get much higher sensitivity, low-modulus porous PDMS sponge, which exhibits perfect compressibility, excellent elasticity and stretchability, has been adopted as the dielectric layer for PC-type pressure sensor.[11,30-33] To date, the flexible capacitor that composed of porous PDMS pyramid arrays, exhibits the maximized compressibility and thus the highest PC sensitivity of 0.55 kPa^{-1}.[10] However, the sensitivity of such type of pressure sensors is difficult to be further improved only by the

microstructure optimization of the adopted dielectric polymer matrix. That is why until recently, only very few successful demonstrations on polymer-based flexible PC sensors.[10,11,30,34,35]

The sensitivity limitation of the PC sensors can be clarified by analyzing the capacitance change during deformation process. It is well known that, for a parallel-plate capacitor with a fixed area, the capacitance (C) is proportional to the ε value of the dielectric layer, and inversely proportional to the distance (d) between two plates.[36] For a PC sensor the dielectric layer is normally composed of porous polymer matrix, which can be considered as the polymer/air composite. As polymer has a similar low ε comparing with that of the air, so the complex ε of the polymer/air composite increases very little during compressing process, thus the change of the distance (Δd) between two palates is solely the dominant factor with regard to capacitance changes (ΔC) upon loading.[37] This is the essential for the sensitivity limitation of a PC sensor. To solve this shortcoming, here we demonstrated that, sensing performance of this type of flexible PC sensor can be effectively improved by the incorporation of ε_H-inorganic nanoparticles into the ε_L-organic matrix. In this situation, the capacitance change can be further boosted by the increase of the complex ε of the composite with gradual closure of the ε_H-particles under external pressure. The combination of the deformation and an increase in the ε of the composited dielectric material enables a significant enhancement of the sensing performance. To date, various materials including carbon nanotubes,[38-41] graphene,[42,43] and metal nanoparticles,[44-46] have been adopted for the incorporation with polymer matrix for the design of novel flexible pressure and strain sensors, but to the best of our knowledge, there is few investigations on ε_H-inorganics/ε_L-organics composited strategy aiming to improve of the sensitivity of the polymer-based PC sensor.

In this paper, we first theoretically clarified the effectiveness of the proposed ε_H-inorganics/ε_L-organics composited strategy, to improving the sensitivity of a polymer-based PC sensor. To verify this thought, we experimentally synthesized $CaCu_3Ti_4O_{12}$ (CCTO) nanocrystals with giant ε, from which an ultra-soft CCTO-PDMS composited sponge was synthesized, *via* a simple cost-effective porogen assisted process.[47-51] By sandwiching this CCTO-PDMS sponge as the dielectric layer between two flexible electrodes, the fabricated PC pressure sensor shows a highly enhanced sensitivity of 1.66 kPa^{-1} in a range of 0-640 Pa, and a responding time of 33 ms. The sensitivity is much higher than that of the fabricated pure PDMS sponge based PC sensor, and also the record reports recently.[2,52] This effective sensing enhancement *via* ε_H-inorganics/ε_L-organics composited strategy provides an enlightened reference for the exploration of other high-sensitive polymer-based flexible PC pressure sensor.[53] Besides, the versatile functionalities such as recording pulse waveforms, detection of bending and twisting forces, producing Morse code, have been investigated, demonstrating its wide promising applications in the field of wearable electronics.

2. SIMULATION

For a further semi-quantitative clarification of the proposed strategy, we simulated the $\Delta C \sim \Delta d$ dependence of a PC sensor, by constructing and simulating a $\varepsilon_H/\varepsilon_L$ composited sponge three dimensional (3D) model of the device using Ansoft Maxwell's software. In the 3D structure, the dielectric layer between two metal plates is composed of ε_H-rigid balls that are uniformly distributed in a ε_L-porous matrix, forming a compressible composited sponge. To solve this variable capacitor model, electrostatic field and voltage excitation source are adopted in the solver. The maximum number of iterations is set as 10, with the error requirement < 0.05%. The thickness of the porous dielectric layer is set as a variable parameter with an initial value of 4

mm and a porosity of 80%. The ε of the matrix is set as 3, which is of the same magnitude to that of PDMS and other polymers. The diameter of the pores and the rigid balls is set as 0.5 mm and 0.01 mm, respectively. The volume ratio of the rigid balls to the matrix is set as 5%. For each round of the simulation, different ε value of the rigid balls that varies from 200 to 10000 is adopted, respectively, to evaluate the influence of the ε value of the rigid balls on the deformation-capacitance dependence of the variable capacitor.

3. EXPERIMENTAL SECTION

3.1. Materials. Analytical reagent calcium nitrate tetrahydrate ($Ca(NO_3)_2 \cdot 4H_2O$), copper acetate ($Cu(CH_3COO)_2 \cdot H_2O$), tetrabutyl titanate ($C_{16}H_{36}O_4Ti$), polyvinylpyrrolidone (PVP, K30), ethylene glycol monomethyl ether ($C_5H_{10}O_3$), ethanol, and acetic acid ($C_2H_4O_2$), are purchased from Chengdu Kelong Chemical Co., Ltd. Dow Corning Sylgard 184 is adopted as the prepolymer for PDMS. Silane coupling agent (KH550) is purchased from Creation of the Nanjing Chemical Additives Co., Ltd.

3.2. Synthesis of CCTO nanoparticles. All the reagents were used as obtained without further purification. 1 mmol calcium nitrate tetrahydrate, 3 mmol copper acetate, and 1.2 ml tetrabutyl titanate are mixed in a beaker. Ethylene glycol monomethyl ether 12 ml and acetic acid 0.4 ml are added into the beaker and mixed by vigorously stirring until it becomes into a transparent emerald-green Solution. The solution is then spinning into microfibers *via* a homemade electrospinning set-up. During the electrospinning process a high voltage of 10 kV is loaded between a 10 cm-separated syringe needle and collector setup. Then after sintered at 900 ^{o}C in the atmosphere for 2 hours, the precursor microfibers are transformed into CCTO nanoparticles aggregate. For the test of the dielectric property, CCTO ceramic pellet is synthesized, by sintering the pressed CCTO nano-aggregate at 1050 ^{o}C for 2 hours.

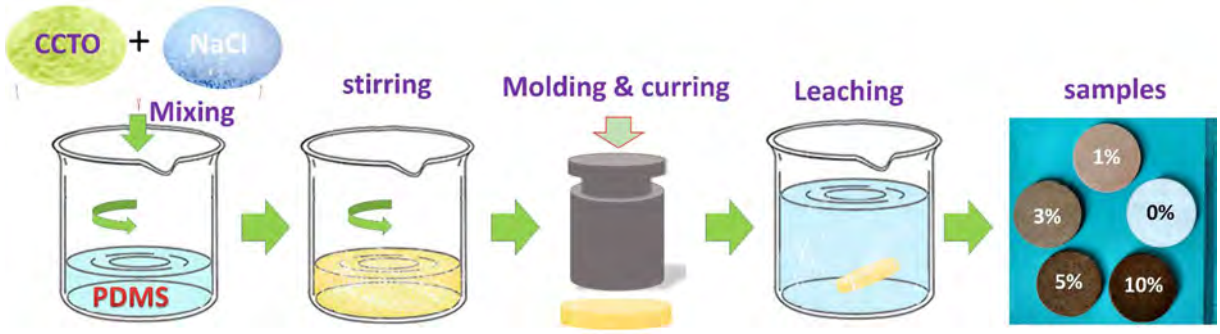

Figure 1. Schematic illustration of the synthetic procedure for CCTO-PDMS composited sponge.

3.3. Synthesis of pure PDMS and CCTO-PDMS porous sponges. The whole synthetic process is illustrated in Figure 1. A two-component (weight ratio of 10:1) Dow Corning Sylgard 184 is adopted as the prepolymer for PDMS. A porogen assisted process by using NaCl powder as the sacrifice is adopted for the synthesis of the pure PDMS and CCTO-PDMS composited sponge. Before incorporation of CCTO into PDMS, CCTO nanoparticles were modified by mixing and grinding with 1 wt% KH550 in ethanol. Then the dried and modified CCTO nanoparticles of different weight ratio (0 wt%, 1 wt%, 3 wt%, 5 wt%, and 10 wt%, respectively) were mixed with certain amount of PDMS prepolymer by vigorous stirring for 1 hour, following high-energy ultrasonicating (950 W, SCIENTZ-IID, Nibo Scientz Biotechnology CO,. LTD) for 30 mins, to reach a thoroughly dispersion. Then certain amount of NaCl powder (200 mesh) was added into the above dispersion with vigorous stirring to form a thick paste. The paste was then pressed into round tablet and cured by heating in 110 ^{o}C for 1 hour. After that, NaCl was leached out by immersing in water for 30 hours, with changing the water every 10 hours. An elastic sponge was obtained at last, by drying at 100 ^{o}C for 2 hours. To evaluate the porosity effect on the mechanical and sensing performaces, both pure PDMS and CCTO-PDMS sponges with varied porosity of 70%, 80%, and 85% were obtained by adjusting the volume ratio of NaCl to PDMS

prepolymer. The porosity (P_o) is calculated by: $P_o = V_{NaCl}/(V_{NaCl} + V_{PDMS})$, in which V_{NaCl} and V_{PDMS} is the volume of the adopted NaCl powder and PDMS, respectively.

3.4. Characterization and Measurement. X-ray diffraction (XRD) was performed on a Bruker DX-1000 diffractometer with Cu K_α radiation (λ=1.54182 Å). Scanning electron microscope (SEM) and the energy dispersive spectroscopy (EDS) were recorded on a Hitachi S-4800. Transmission electron microscopy (TEM) was carried out using a CarlZeiss SMT PteLtd., Libra 200 FE. Dielectric properties are measured on Agilent 4294A Precision Impedance Analyze. The capacitance change respect to the loading pressure is tested *via* the AD7746 capacitance-to-digital converter (National Instruments) board mounted on a home-made setup. Mechanical properties including quasi-static and dynamic compression were carried out on Zwick/Roell Z010 with a load cell of 1KN. The compressing speed is 5mm/min, and quasi-static compression is halted when the strain reaches 50%.

4. RESULTS AND DISCUSSION

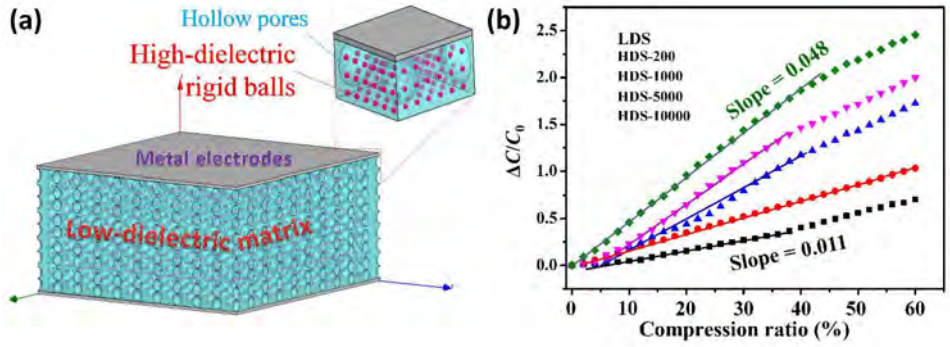

Figure 2. (a) A 3D model adopted for the simulation of the deformation-capacity dependence of a porous PC sensor. In the model the porosity is set as 80%, and the volume ratio of the ε_H-rigid ball to the ε_L-matrix is set as 5%. (b) The simulated results of $\Delta C/C_0$ with respect to deformation based on the 3D model. The simulated samples are ε_L-sponge (LDS), and that incorporated with

the ε_H-balls with varied ε of 200 (HDS-200), 1000 (HDS-1000), 5000 (HDS-5000), and 10000 (HDS-10000), respectively.

Based on the 3D model as illustrated in Figure 2(a), the simulated results in Figure 2(b) clearly demonstrates that, $\Delta C/C_0$ with respect to the deformation, which also indicates the sensitivity of the PC sensor, is highly enhanced by the incorporation of ε_H-phase into the porous ε_L-matrix. That is, the responding slope, which is 0.011 for pure ε_L-sponge (LDS), gains a great promotion with an increment of 363% (increases to 0.048) by incorporation of ε_H-rigid balls (HDS-10000 in Figure 2b), implying significant sensitivity enhancement induced by ε_H-phase incorporation.

Therefore, for the purpose of sensitivity enhancement, ceramics with high ε such as CCTO[54,55] would be one of the best candidates to be incorporated into the low dielectric polymer matrix layer in a flexible PC sensor. It should be noted that, to synthesize an inorganics/organics composite with perfect elasticity and elastic durability that is demanded for a flexible PC sensor, the adopted inorganics should be ultrafine, e.g., composed of micro- or even nano- particles, and the interface between the inorganics/organics should be chemically modified.[56] Besides, the concentration of the inorganics content in the inorganics/organics composite should also be considered.[56,57]

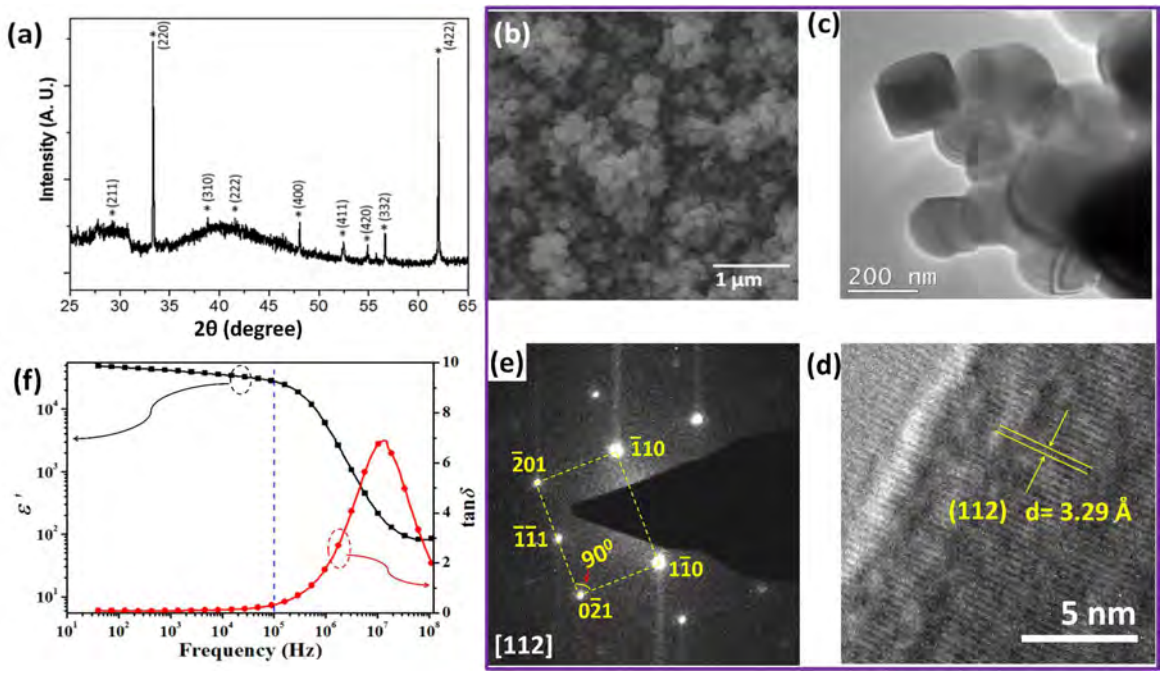

Figure 3. (a) XRD, (b) SEM, and (c) TEM, (d) high-resolution (HR)-TEM, and (e) selected area diffraction (SEAD) characterization of the synthesized CCTO nanoparticles. (f) the dielectric spectra of the synthesized CCTO ceramic tablet.

Here we successfully synthesized an ultrafine CCTO powder that is composed of CCTO nanocrystals. As can be seen from the XRD (Figure 3a), all the main peaks observed in the XRD pattern can be indexed on the basis of JCPDF Card No. 21-0140 of CCTO, confirming the cubic CCTO phase formation. SEM image shown in Figure 3b clearly demonstrates that the synthesized CCTO powder is composed of CCTO nanoparticles which are aggregating into cluster. TEM (Figure 3c) further presents a typical cubic-shape CCTO nanocrystals with an average particle size of ~150 nm. The HR-TEM image (Figure 3d) clearly demonstrates a single-crystalline characteristic with a interplanar spacing of 3.29 Å that corresponds to the (112) plane of cubic CCTO. The corresponding SEAD (Figure 3e) matches exactly with the diffraction pattern that is obtained from [112] incident direction of a cubic CCTO single crystal. The corresponding dielectric spectroscopy of the resulted CCTO ceramic exhibits a giant dielectric

constant (ε') of >30000 below 10^5 Hz, which is coincide with our previous report.[54] According to our simulation results, the incorporation of CCTO nanoparticles with such a giant ε into a polymer matrix will enhance the sensitivity of the polymer-based flexible PC sensor. Besides, the nanosized distribution of the synthesized CCTO nanocrystals would also be good to the maintenance of the elasticity and compressive durability of the formed CCTO-PDMS composite.

Micromorphological characterizations and mechanical properties demonstration of the synthesized CCTO-PDMS sponge are shown in Figure 4. As can be seen from Figure 4a-f, both pure PDMS and CCTO-PDMS composited sponges exhibit a similar porous morphology. Size of the pores in the sponge is widely distributed, ranging from submicron to tens of micron. Pore's wall of both pure PDMS sponge and CCTO-PDMS sponge are smooth, with only few CCTO nanocrystals tightly connected on PDMS surface in the case of CCTO-3 and CCTO-5 sponge, as observed in Figure 4c-f. Though more CCTO nanoparticles emerge on the micropores' surface of CCTO-10 (Figure S1), these CCTO nanoparticles are also tightly attached on the pore's surface. To further verify the good dispersion of CCTO nanoparticles in PDMS matrix, a piece of non-porous CCTO-PDMS composite with CCTO content of 3 wt% was fabricated, and the corresponding cross-sectional SEM and EDS characterization were obtained. Seeing from the cross-sectional SEM images as shown in Figure 4g-h, CCTO nanoparticles distribute uniformly in the PDMS matrix. Meanwhile, the EDS results (Figure S2) tell that the compositional elements of PDMS such as silicon, oxygen, and carbon coexist with that of CCTO (including Ca, Cu, Ti, as summarized in Table S1), further clarifying good compatibility of CCTO nanoparticles with PDMS matrix. All these results provide strong confirmations for the good distribution of CCTO nanoparticles in PDMS matrix, which can be attributed to perfect interface compatibility that is compromised *via* KH550 interfacial modification between CCTO nanocrystals and PDMS

phase. That is, on one hand, KH550 as a silane-coupling agent molecular binds strongly to PDMS surface by the formation of Si-O-Si bonds; and on the other hand, Si-OH in KH550 molecular can interact with O atoms on CCTO surface due to chemical adsorption such as forming hydrogen bonds.[58] Therefore, strong interaction and good compatibility are induced leading to a good distribution of CCTO nanoparticles in PDMS phase, which in turn guarantee the flexibility, compressibility and cyclical durability of the CCTO-PDMS composited sponge. Mechanical assessments of the fabricated CCTO-PDMS sponge including hanging heavy object (Figure 4i), bending (Figure 4j) and compressing (Figure 4k) clearly demonstrate its good tensile strength, good flexibility, and high compressibility.

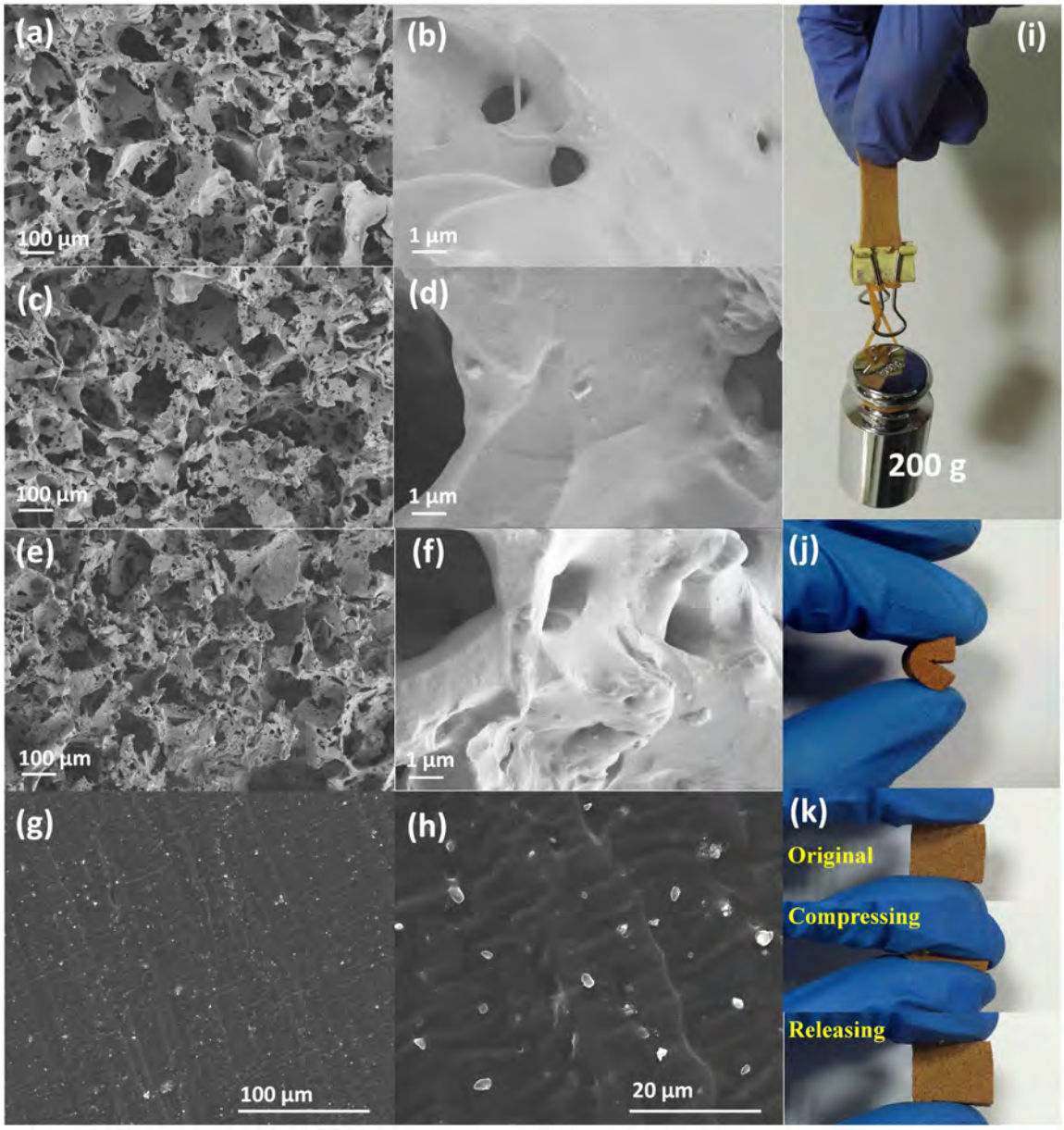

Figure 4. SEM characterization of CCTO-PDMS composited sponge with varied CCTO content of (a, b) 0 % (pure PDMS), (c, d) 3 wt% (CCTO-3), (e, f) 5 wt% (CCTO-5), respectively. (g, h) Cross sectional SEM images of CCTO-PDMS composite. (i-k) Mechanical properties of CCTO-3 demonstrated by hanging heavy objects, bending, and compressing, respectively.

Figure 5 shows the quasi-static compressive and dynamic loading curves of CCTO-PDMS sponge with varied CCTO content. As can be seen from Figure 5a, pure PDMS sponge has the smallest compression modulus of ~3.5 kPa, which is by far below the reported PDMS

sponge[59,60] as well as commercial PU foam.[61] In comparison, compression modulus of CCTO-PDMS sponges increase with the CCTO content, from 6.3 kPa for CCTO-3, increases to 11.5 kPa for CCTO-10. It means that CCTO incorporation increases the rigidity, which is a common phenomenon usually observed in an inorganic-organic composite. Nevertheless, the modulus of CCTO-10 is still smaller than the reported PDMS sponge[59,60] and commercial PU foam,[61] and such a low compression modulus value demonstrates excellent flexibility that will be beneficial to the sensitivity of the resulted PC sensor.

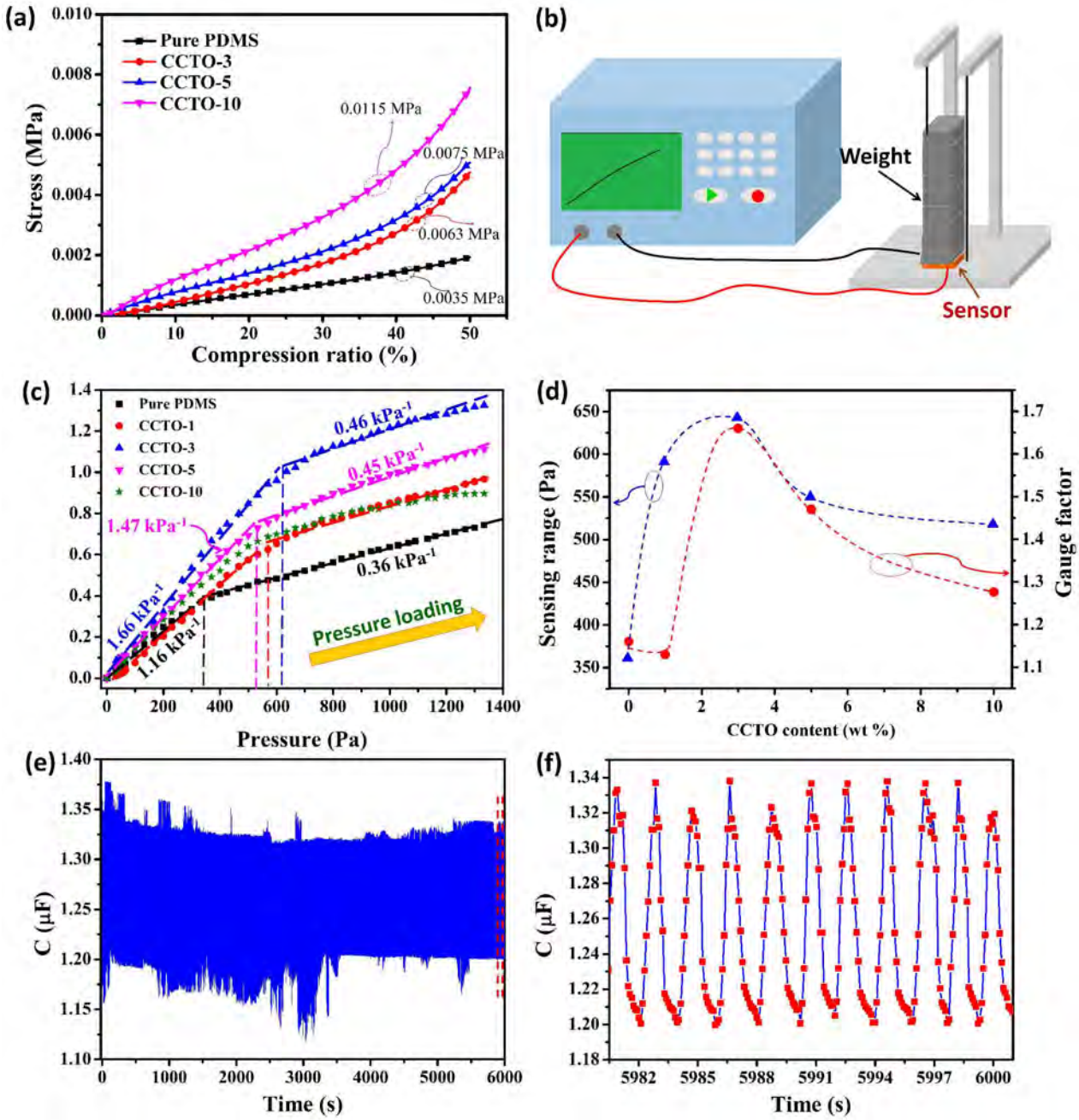

Figure 5. (a) Quasi-static compressing strain-stress curves, (b) set-up used for capacitance-deformation dependence test, (c) relative capacitance changes, and (d) CCTO-content dependent of the sensitivity and sensing ranges of the CCTO-PDMS composited sponge with varied CCTO content, respectively. For the sake of clarity, only the performance parameters of pure CCTO, CCTO-3, and CCTO-5 are specified in (c). (e) Capacitance changes of the sensor as a function of

a >3000 cyclic bending-releasing test. (f) Partial display of the capacitance changes of the selected time zone shown in (e).

Table 1. Summarization of the recently reported representative flexible PC-type sensors with advanced performances in the aspect of gauge factor, sensing range, and responding time.

Materials and structure	Gauge factor (kPa^{-1})	Upper detection limit (Pa)	Responding time (ms)	Ref.
Gold nanowire-impregnated tissue between two thin PDMS	1.14	50 k	17	[2]
Microstructured PDMS layer	0.55	2000	~ several ms	[10]
3D microporous dielectric elastomer	0.601	5000	_	[11]
Elastic CNT fabrics	0.034-0.05	100	<63	[32]
Graphene/PU sponge	0.26	2000	_	[42]
CCTO-PDMS sponge	1.66	640	<33	This work

The capacitance and the relative change of the capacitance respect to the pressure loaded on the CCTO-PDMS-based PC sensor were studied on a home-made setup, as illustrated in Figure 5b. Precise weight is loaded one by one on the sensor surface causing the deformation, meanwhile the corresponding capacitance is recorded using Tonghui TH2832 precision LCR digital bridge (Changzhou Tonghui Electronics Co., Ltd.). Both the capacitance-pressure (C~P) curve and the relative capacitance change respect to the loaded pressure ($\Delta C/C_0$~P) curve show a higher sensitivity of all sensors. Due to much higher ε of CCTO, the capacitance becomes higher with the incorporation of CCTO, as can be seen from the C~P curves shown in Figure S3. Meanwhile, the capacitance increases much faster for CCTO-PDMS sponge. As can be seen more clearly from Figure 5c, the slope of the $\Delta C/C_0$~P curves becomes much higher for CCTO-PDMS sponge, meaning highly improved sensing performance induced by CCTO incorporation. It is reasonable that, the sensitivity of the PC sensor is determined by the elastic modulus of the dielectric sponge, as well as the as the ε increment during compressing. As both pure PDMS and CCTO-PDMS sponges have an ultra-low and similar modulus, the caused deformation (Δd) will

be very close under the same compressing pressure, therefore in this situation the sensitivity of the PC sensor is mainly determined by the ε increment. Comparing with pure PDMS sponge, the same deformation will cause a much faster ε boosting in CCTO-PDMS dielectric layer that is induced by the gradual closure of the ε_H-CCTO nanoparticles during compressing.

Besides, the $\Delta C/C_0 \sim P$ curves show two different stages with different compressive behaviors upon an increase in the pressure input, which is similar to most of the previous reported flexible PR or PC sensors.[2,11,16,19,41,42] As can be seen that, pure PDMS sponge gives the sensitivity of 1.16 kPa^{-1} but in a very narrow pressure range of 0-320 Pa, after that the sensitivity downs to 0.36 kPa^{-1}. Comparatively, CCTO-3 gives the best comprehensive sensing performance, that is, it exhibits the highest sensitivity of 1.66 kPa^{-1} in a pressure range of 0-640 Pa, and 0.46 kPa^{-1} after that. This highly sensitive pressure-sensing capability in a wider pressure range, which is originated from the significant compressibility as well as the ε boosting induced by the gradual closure of the CCTO nanoparticles during compressing, is the best among the PC-type sensors reported recently.[2,52] The representative recently reported flexible PC-type sensors with advanced performances are summarized in Table 1. Figure 5c summarizes the CCTO-content dependent of the gauge factor and sensing range of the CCTO-PDMS composited sponge with varied CCTO content. It indicates that, further increase of CCTO content (e.g., CCTO-5 and CCTO-10) leads to a degradation of the sensitivity with a decreased $\Delta C/C_0 \sim P$ slope. Such a re-diminished sensing performance in CCTO-5 and CCTO-10 can be understood by comprehensive consideration of the mechanical and dielectric characteristics of the CCTO-PDMS sponge. According to our theoretical analysis and the simulated results, ε_H-CCTO incorporation do enhance the sensing performance of a PC sensor, but excessive content of CCTO (e.g., 5-10 wt%) in PDMS leads to a higher modulus (Figure 5a), which will in turn diminish the $\Delta C/C_0 \sim P$

response. The effect of the porosity on the sensing performances was also evaluated. It is found that, lower porosity (e.g., 70%) leads to a poorer performance with lower gauge factor (Figure S4), while higher porosity causes the CCTO-PDMS sponges much weaker mechanical properties such as easily to be broken under cyclic twisting for tens of times. Nevertheless, the highest sensitivity obtained in CCTO-3 sponge will definitely render the sensor robust ability to precisely capture any tiny pressure changes such as wrist pulse.

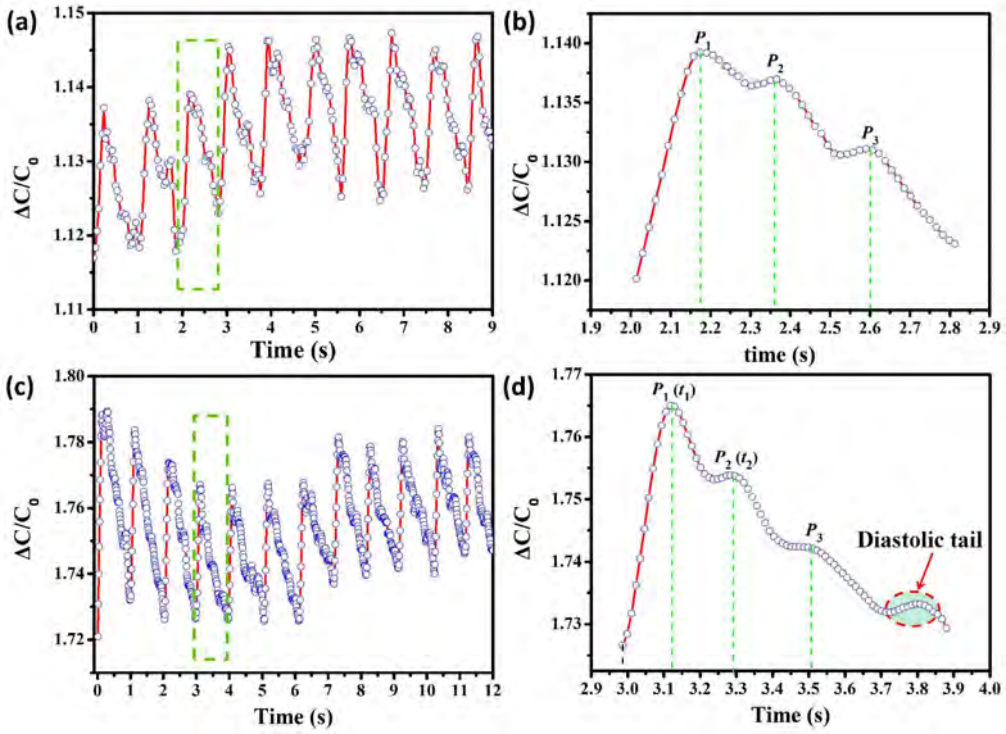

Figure 6. Pulse waves of the radial artery waves of the same female in his 30s, recorded by pure PDMS (a, b), and CCTO-3 based PC sensor (c, d), respectively.

The sensing functionality and fidelity of our high sensitive CCTO-PDMS-based PC sensor is illustrated by demonstrating its ability to capture the waves of a continuous wrist pulse signals. During the test, the sensor is attached and fasten by a elastic belt to an adult man's wrist, just above the radial artery as it is usually done in arterial tonometry (Video S1). The waveforms shown in Figure 6 present an accurate recording of wrist pulse over several pulse periods. For

both pure PDMS and CCTO-3 sponge, a characteristic pulse pressure shape was obtained with three clearly distinguishable peaks (P1, P2 and P3), as shown in Figure 6b and Figure 6d.[26] Comparatively, however, signals reading from CCTO-3 is much more distinguishable than that from pure PDMS sponge, implying an enhanced sensing performance induced by the incorporation of CCTO with high ε. For example, the difference of (P_1-P_2) is larger in CCTO-3, from which one can easily derive two of the most commonly used parameters for arterial stiffness diagnosis, that is, the time delay between P_1 and P_2 $\Delta T_{DVP} = t_2 - t_1$, and the radial augmentation index $AI_r = P_2/ P_1$.[62] For the test person, ΔT_{DVP} = 165 ms and AI_r = 69% have been determined, which are characteristics for a healthy adult in his mid-thirties of age. Moreover, a diastolic tail of the pulse pressure wave can be exclusively resolved in CCTO-3 sensor,[52] as clearly indicated in Figure 6d, implying high fidelity and accuracy of the captured wrist pulse signals, which will in turn be especially beneficial to an correct analysis of the complicated pulse waveforms, and hence could potentially be applied for more detailed medical heart diagnostics.[26,62-64]

The versatile functionality of our CCTO-PDMS based PC pressure is further illustrated by demonstrating its response to other types of mechanical forces including cyclical twisting, bending, and quick pressing. Remarkably, the response curves are characteristic for twisting (Figure 7a) and bending (Figure 7b), respectively, further demonstrating the high sensitivity of our CCTO-PDMS based PC sensor. As a specific application demonstration, our sensor has been successfully applied for monitoring the robotic joint movement. As shown in Figure 7c and Video S2, a sensor attached on a robotic joint outputs stable periodic signals under cyclical torsional forces. Dynamic loading response shown in Figure 7d, Figure S5 and Video S3 clearly demonstrate that, our CCTO-PDMS sponge sensor can keep up a 2000 mm/min cyclical

compressing speed with a stable output. High speed of the compression-recovery means quick response to fast pressure changes.[2,52] For a quick-responding demonstration, fast cyclical finger-press is loaded on the device to produce Morse code. As can be seen from Figure 7e and f, this sensor gives sharp signals with a negligible responding time of as short as 33 ms. These versatile sensing functionalities have many potential applications in wearable devices, robotics, flexible electronics, etc.

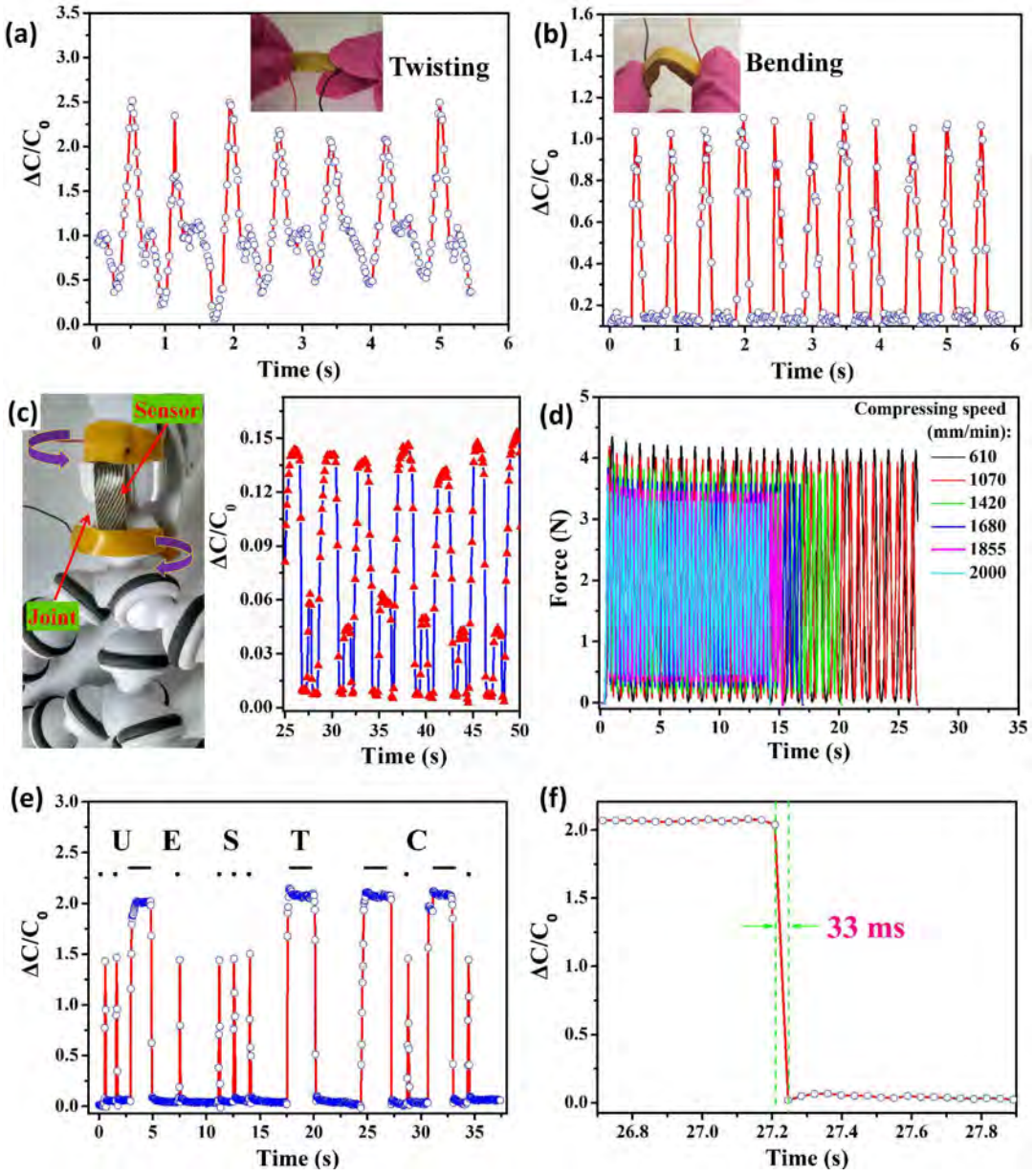

Figure 7. Versatile performing characteristics of CCTO-3 PC sensor: (a) twisting response at a twisting angle of 60°, (b) cyclical bending load with bend radii of ~5 mm, (c) monitoring of the robotic joint movement, (d) cyclical compressing response, (e) quick pressing to produce Morse code, and (f) responding time evaluation from the quick pressing response curve.

5. CONCLUSION

In summary, we theoretically proposed an effective strategy for the improvement of the sensitivity of the PC pressure sensor, by a simple incorporation of ε_H-inorganics into the flexible ε_L-organic porous matrix. Experimentally, by using CCTO nanocrystals with a giant ε as the dopant and ε_L-PDMS as the matrix, an ultra-soft CCTO-PDMS sponge was synthesized *via* a simple porogen assisted process. The CCTO-PDMS based pressure sensor shows a highly enhanced sensitivity of 1.66 kPa^{-1} at 0-640 Pa and a response time of 33 ms. Such a sensitivity is much higher than that of a pure PDMS sponge based device, and those of any other PC sensors reported recently, demonstrating an highly enhanced sensing performance induced by ε_H-CCTO incorporation. This sensitivity enhancement achieved by ε_H-inorganics/ε_L-organics composited strategy provides an effective route to other novel flexible PC sensors. In practical applications, the fabricated CCTO-PDMS based PC sensor demonstrate versatile potential applications, such as recording wrist pulse wave with fine accurate and fidelity, bending and twisting detection, Moss code simulating. The low-cost for production in conjunction with its superior sensitivity, robustness of the functional versatility and mechanical flexibility make the CCTO-PDMS based pressure sensor wide promising applications in wearable devices, flexible electronics, robotics, etc.

ASSOCIATED CONTENT

Supporting Information.

The following files are available free of charge.

Figure S1: SEM characterization of the composited sponge of CCTO-10; Figure S2: EDS of CCTO-PDMS composite with 3 wt% CCTO; Figure S3: Capacitance-pressure dependence of PC sensors with varied CCTO content; Figure S4: Capacitance-pressure dependence of PC sensors with 70% porosity and varied CCTO content; Figure S5: Cyclical compressing response of CCTO-5, and CCTO-10, at varied compressing speed. (PDF)

Video S1: Continuous recording of the wrist pulse signals. (MP4)

Video S2: Real-time monitoring of the robot joint movement. (MP4)

Video S3: Cyclical compressing test of CCTO-3 at a speed of 2000 mm/min. (MP4)

AUTHOR INFORMATION

Corresponding Author

*yuanqiangsong@uestc.edu.cn.

*michael@hit.edu.cn.

*hwzhang@uestc.edu.cn.

Author Contributions

The manuscript was written through contributions of all authors. All authors have given approval to the final version of the manuscript.

Notes

The authors declare no competing financial interest.

ACKNOWLEDGMENT

This work is financially supported by the National Natural Science Foundation of China with a grant number of 51402042, Science and Technology Support Program of Sichuan Provincial Science and Technology Department (no. 2016GZ0248), and the Fundamental Research Funds for the Central Universities of China ZYGX2013J117.

REFERENCES

(1) Zang, Y.; Zhang, F.; Di, C.-a.; Zhu, D. Advances of Flexible Pressure Sensors Toward Artificial Intelligence and Health Care Applications. *Mater. Horiz.* **2015**, *2*, 140-156.
(2) Gong, S.; Schwalb, W.; Wang, Y.; Chen, Y.; Tang, Y.; Si, J.; Shirinzadeh, B.; Cheng, W. A Wearable and Highly Sensitive Pressure Sensor with Ultrathin Gold Nanowires. *Nat. Commun.* **2014**, *5*, 3132:1-8.
(3) Cheng, M. Y.; Huang, X. H.; Ma, C. W.; Yang, Y. J. A Flexible Capacitive Tactile Sensing Array with Floating Electrodes. *J. Micromech. Microeng.* **2009**, *19*, 115001:1-10.
(4) Someya T.; Sekitani T.; Iba S.; Kato Y.; Kawaguchi H.; Sakurai T. A Large-Area, Flexible Pressure Sensor Matrix with Organic Field-Effect Transistors for Artificial Skin Applications. *Proc. Natl. Acad. Sci.* **2004**, *101*, 9966-9970.
(5) Yang, Y.; Zhang, H.; Lin, Z. H.; Zhou, Y. S.; Jing, Q.; Su, Y.; Yang, J.; Chen, J.; Hu, C.; Wang, Z. L. Human Skin Based Triboelectric Nanogenerators for Harvesting Biomechanical Energy and as Self-Powered Active Tactile Sensor System. *ACS Nano* **2013**, *7*, 9213-9222.
(6) Wang, Z. L.; Wu, W. Nanotechnology-Enabled Energy Harvesting for Self-Powered Micro-/Nanosystems. *Angew. Chem.* **2012**, *51*, 11700-11721.
(7) Hu, Y.; Yang, J.; Jing, Q.; Niu, S.; Wu, W.; Wang, Z. L. Triboelectric Nanogenerator Built on Suspended 3D Spiral Structure as Vibration and Positioning Sensor and Wave Energy Harvester. *ACS Nano* **2013**, *7*, 10424-10432.
(8) Chen, Z.; Wang, Z.; Li, X.; Lin, Y.; Luo, N.; Long, M.; Zhao, N.; Xu, J. B. Flexible Piezoelectric-Induced Pressure Sensors for Static Measurements Based on Nanowires/Graphene Heterostructures. *ACS Nano* **2017**, *11*, 4507-4513.
(9) Wu, X.; Han, Y.; Zhang, X.; Zhou, Z.; Lu, C. Large-Area Compliant, Low-Cost, and Versatile Pressure-Sensing Platform Based on Microcrack-Designed Carbon Black@Polyurethane Sponge for Human–Machine Interfacing. *Adv. Funct. Mater.* **2016**, *26*, 6246-6256.
(10) Mannsfeld, S. C. B.; Tee, B. C. K.; Stoltenberg, R. M.; Chen, C. V. H. H.; Barman, S.; Muir, B. V. O.; Sokolov, A. N.; Reese, C.; Bao, Z. Highly sensitive flexible pressure sensors with microstructured rubber dielectric layers. *Nat. Mater.* **2010**, *9*, 859-864.
(11) Kwon, D.; Lee, T.-I.; Shim, J.; Ryu, S.; Kim, M. S.; Kim, S.; Kim, T.-S.; Park, I. Highly Sensitive, Flexible, and Wearable Pressure Sensor Based on a Giant Piezocapacitive Effect of

Three-Dimensional Microporous Elastomeric Dielectric Layer. *ACS Appl. Mater. Interfaces* **2016**, *8*, 16922-16931.
(12) Kirankumar, B.; Basavaprabhu, G. S. A Critical Review of MEMS Capacitive Pressure Sensors. *Sensors & Transducers* **2015**, *187*, 120-128.
(13) Boutry, C. M.; Nguyen, A.; Lawal, Q. O.; Chortos, A.; Rondeau-Gagné, S.; Bao, Z. A Sensitive and Biodegradable Pressure Sensor Array for Cardiovascular Monitoring. *Adv. Mater.* **2015**, *27*, 6954-6961.
(14) Tee, B. C. K.; Chortos, A.; Dunn, R. R.; Schwartz, G.; Eason, E.; Bao, Z. Tunable Flexible Pressure Sensors using Microstructured Elastomer Geometries for Intuitive Electronics. *Adv. Funct. Mater.* **2014**, *24*, 5427-5434.
(15) Xu, S.; Yu, W.; Jing, M.; Huang, R.; Zhang, Q.; Fu, Q. Largely Enhanced Stretching Sensitivity of Polyurethane/Carbon Nanotube Nanocomposites via Incorporation of Cellulose Nanofiber. *J. Phys. Chem. C* **2017**, *121*, 2108-2117.
(16) Liu, H.; Dong, M.; Huang, W.; Gao, J.; Dai, K.; Guo, J.; Zheng, G.; Liu, C.; Shen, C.; Guo, Z. Lightweight Conductive Graphene/thermoplastic Polyurethane Foams with Ultrahigh Compressibility for Piezoresistive Sensing. *J. Mater. Chem. C* **2017**, *5*, 73-83.
(17) Natarajan, T. S.; Eshwaran, S. B.; Stöckelhuber, K. W.; Wießner, S.; Pötschke, P.; Heinrich, G.; Das, A. Strong Strain Sensing Performance of Natural Rubber Nanocomposites. *ACS Appl. Mater. Interfaces* **2017**, *9*, 4860-4872.
(18) Ke, K.; Pötschke, P.; Wiegand, N.; Krause, B.; Voit, B. Tuning the Network Structure in Poly(vinylidene fluoride)/Carbon Nanotube Nanocomposites Using Carbon Black: Toward Improvements of Conductivity and Piezoresistive Sensitivity. *ACS Appl. Mater. Interfaces* **2016**, *8*, 14190-14199.
(19) Zheng, Y.; Li, Y.; Li, Z.; Wang, Y.; Dai, K.; Zheng, G.; Liu, C.; Shen, C. The effect of Filler Dimensionality on the Electromechanical Performance of Polydimethylsiloxane based Conductive Nanocomposites for Flexible Strain Sensors. *Compos. Sci. Technol.* **2017**, *139*, 64-73.
(20) You, B.; Han, C. J.; Kim, Y.; Ju, B.-K.; Kim, J.-W. A Wearable Piezocapacitive Pressure Sensor with a Single Layer of Silver Nanowire-based Elastomeric Composite Electrodes. *J. Mater. Chem. A* **2016**, *4*, 10435-10443.
(21) Peng, S.; Hartley, P. G.; Hughes, T. C.; Guo, Q. Controlling Morphology and Porosity of Porous Siloxane Membranes through Water Content of Precursor Microemulsion. *Soft Matter* **2012**, *8*, 10493-10501.
(22) Wang, M.; Zhang, K.; Dai, X.-X.; Li, Y.; Guo, J.; Liu, H.; Li, G.-H.; Tan, Y.-J.; Zeng, J.-B.; Guo, Z. Enhanced Electrical Conductivity and Piezoresistive Sensing in Multi-wall Carbon Nanotubes/polydimethylsiloxane Nanocomposites via the Construction of a Self-segregated Structure. *Nanoscale* **2017**, *9*, 11017-11026.
(23) Majid Kazemian, A.; Sulabha, K. K. Giant Piezoresistive Response in Zinc–polydimethylsiloxane Composites under Uniaxial Pressure. *J. Phys. D: Appl. Phys.* **2008**, *41*, 135405:1-7.
(24) Jung, J.; Kim, M.; Choi, J. K.; Park, D. W.; Shim, S. E. Piezoresistive effects of Copper-Filled Polydimethylsiloxane Composites near Critical Pressure. *Polymer* **2013**, *54*, 7071-7079.
(25) Jung, J.; Lee, K. M.; Baeck, S.-H.; Shim, S. E. Piezoresistive Behavior of a Stretchable Carbon Nanotube-interlayered Poly(dimethylsiloxane) Sheet with a Wrinkled Structure. *RSC Adv.* **2015**, *5*, 73162-73168.

(26) Tai, Y.; Kanti Bera, T.; Yang, Z.; Lubineau, G. Leveraging a Temperature-tunable, Scale-like Microstructure to Produce Multimodal, Supersensitive Sensors. *Nanoscale* **2017**, *9*, 7888-7894.
(27) Zha, J.-W.; Huang, W.; Wang, S.-J.; Zhang, D.-L.; Li, R. K. Y.; Dang, Z.-M. Difunctional Graphene–Fe_3O_4 Hybrid Nanosheet/Polydimethylsiloxane Nanocomposites with High Positive Piezoresistive and Superparamagnetism Properties as Flexible Touch Sensors. *Adv. Mater. Interfaces* **2015**, *3*, 1500418:1-9.
(28) Lee, X.; Yang, T. T.; Li, X.; Zhang, R. J.; Zhu, M. Flexible Graphene Woven Fabrics for Touch Sensing. *Appl. Phys. Lett.* **2013**, *102*, 163117:1-4.
(29) Lee, J.; Kim, S.; Lee, J.; Yang, D.; Park, B. C.; Ryu, S.; Park, I. A Stretchable Strain Sensor Based on A Metal Nanoparticle Thin Film for Human Motion Detection. *Nanoscale* **2014**, *6*, 11932: 2624-2627.
(30) Lei, K. F.; Lee, K.-F.; Lee, M.-Y. Development of A Flexible PDMS Capacitive Pressure Sensor for Plantar Pressure Measurement. *Microelectron Eng.* **2012**, *99*, 1-5.
(31) Lee, D.-W.; Choi, Y.-S. A Novel Pressure Sensor with A PDMS Diaphragm. *Microelectron Eng.* **2008**, *85*, 1054-1058.
(32) Kim, S. Y.; Park, S.; Park, H. W.; Park, D. H.; Jeong, Y.; Kim, D. H. Highly Sensitive and Multimodal All-Carbon Skin Sensors Capable of Simultaneously Detecting Tactile and Biological Stimuli. *Adv. Mater.* **2015**, *27*, 4178-4185.
(33) King, M. G.; Baragwanath, A. J.; Rosamond, M. C.; Wood, D.; Gallant, A. J. Porous PDMS Force Sensitive Resistors. *Procedia Chem.* **2009**, *1*, 568-571.
(34) Castillo-Castro, T.del; Castillo-Ortega, M. M.; Encinas, J. C.; Herrera Franco, P. J.; Carrillo-Escalante, H. J. Piezo-resistance Effect in Composite Based on Cross-linked Polydimethylsiloxane and Polyaniline: Potential Pressure Sensor Application. *J. Mater. Sci.* **2012**, *47*, 1794-1802.
(35) Achraf, K.; Skandar, B.; Libor, R.; Alain, S.; Fathi, J. Micro-structured PDMS Piezoelectric Enhancement Through Charging Conditions. *Smart Mater. Struct.* **2016**, *25*, 105027:1-14.
(36) Grove, T. T.; Masters, M. F.; Miers, R. E. Determining Dielectric Constants Using a Parallel Plate Capacitor. *Am. J. Phys.* **2005**, *73*, 52-56.
(37) Nishiyama, H.; Nakamura, M. Form and Capacitance of Parallel-Plate Capacitors. *IEEE Trans. Compon. Packag. Manuf. Technol.* **1994**, *17*, 477-484.
(38) Lipomi, D. J.; Vosgueritchian, M.; Tee, B. C. K.; Hellstrom, S. L.; Lee, J. A.; Fox, C. H.; Bao, Z. Skin-like Pressure and Strain Sensors Based on Transparent Elastic Films of Carbon Nanotubes. *Nat. Nano.* **2011**, *6*, 788-792.
(39) Cohen, D. J.; Mitra, D.; Peterson, K.; Maharbiz, M. M. A Highly Elastic, Capacitive Strain Gauge Based on Percolating Nanotube Networks. *Nano Lett.* **2012**, *12*, 1821-1825.
(40) Yamada, T.; Hayamizu, Y.; Yamamoto, Y.; Yomogida, Y.; Izadi-Najafabadi, A.; Futaba, D. N.; Hata, K. A Stretchable Carbon Nanotube Strain Sensor for Human-motion Detection. *Nat. Nano.* **2011**, *6*, 296-301.
(41) Zhou, J.; Yu, H.; Xu, X.; Han, F.; Lubineau, G. Ultrasensitive, Stretchable Strain Sensors Based on Fragmented Carbon Nanotube Papers. *ACS Appl. Mater. Interfaces* **2017**, *9*, 4835-4842.
(42) Yao, H.-B.; Ge, J.; Wang, C.-F.; Wang, X.; Hu, W.; Zheng, Z.-J.; Ni, Y.; Yu, S.-H. A Flexible and Highly Pressure-Sensitive Graphene-Polyurethane Sponge Based on Fractured Microstructure Design. *Adv. Mater.* **2013**, *25*, 6692:1-7.

(43) Saha, B.; Baek, S.; Lee, J. Highly Sensitive Bendable and Foldable Paper Sensors Based on Reduced Graphene Oxide. *ACS Appl. Mater. Interfaces* **2017**, *9*, 4658-4666.
(44) Maheshwari, V.; Saraf, R. F. High-Resolution Thin-Film Device to Sense Texture by Touch. *Science* **2006**, *312*, 1501-1504.
(45) Sangeetha, N. M.; Decorde, N.; Viallet, B.; Viau, G.; Ressier, L. Nanoparticle-Based Strain Gauges Fabricated by Convective Self Assembly: Strain Sensitivity and Hysteresis with Respect to Nanoparticle Sizes. *J. Phys. Chem. C* **2013**, *117*, 1935-1940.
(46) Segev-Bar, M.; Landman, A.; Nir-Shapira, M.; Shuster, G.; Haick, H. Tunable Touch Sensor and Combined Sensing Platform: Toward Nanoparticle-based Electronic Skin. *ACS Appl. Mater. Interfaces* **2013**, *5*, 5531-5541.
(47) Juchniewicz, M.; Stadnik, D.; Biesiada, K.; Olszyna, A.; Chudy, M.; Brzózka, Z.; Dybko, A. Porous Crosslinked PDMS-microchannels Coatings. *Sensor. Actuat. B-Chem.* **2007**, *126*, 68-72.
(48) Oh, M.-J.; Ryu, T.-K.; Choi, S. W. Hollow Polydimethylsiloxane Beads with a Porous Structure for Cell Encapsulation. *Macromol. Rapid Commun.* **2013**, *34*, 1728-33.
(49) Si, J.; Cui, Z.; Xie, P.; Song, L.; Wang, Q.; Liu, Q.; Liu, C. Characterization of 3D Elastic Porous Polydimethylsiloxane (PDMS) Cell Scaffolds Fabricated by VARTM and Particle Leaching. *J. Appl. Polym. Sci.* **2016**, *133*, 42909-42918.
(50) Zhang, D.; Burkes, W. L.; Schoener, C. A.; Grunlan, M. A. Porous Inorganic–organic Shape Memory Polymers. *Polymer* **2012**, *53*, 2935-2941.
(51) Macintyre, F. S.; Sherrington, D. C. Control of Porous Morphology in Suspension Polymerized Poly(Divinylbenzene) Resins Using Oligomeric Porogens. *Macromolecules* **2004**, *37*, 7628-7636.
(52) Schwartz, G. T., Benjamin C.-K.; Mei, J.- G.; Appleton, Anthony L.; Kim, Do Hwan; Wang, H.-L.; Bao, Z.-N. Flexible Polymer Transistors with High Pressure Sensitivity for Application in Electronic Skin and Health Monitoring. *Nat. Commun.* **2013**, *4*, 1859-1864.
(53) Sharma, S. K.; Gaur, H.; Kulkarni, M.; Patil, G.; Bhattacharya, B.; Sharma, A. PZT–PDMS Composite for Active Damping of Vibrations. *Compos. Sci. Technol.* **2013**, *77*, 42-51.
(54) Mu, C.-H.; Liu, P.; He, Y.; Zhou, J.-P.; Zhang, H.-W. An Effective Method to Decrease Dielectric Loss of $CaCu_3Ti_4O_{12}$ Ceramics. *J. Alloys Compd.* **2009**, *471*, 137-141.
(55) Mu, C. -H; Song, Y.; Wang, H.; Wang, X. Room Temperature Magnetic and Dielectric Properties of Cobalt Doped $CaCu_3Ti_4O_{12}$ Ceramics .*J. Appl. Phys.* **2015**, *117*, 17B723:1-4.
(56) Fu, S.-Y.; Feng, X.-Q.; Lauke, B.; Mai, Y.-W. Effects of Particle Size, Particle/Matrix Interface Adhesion and Particle Loading on Mechanical Properties of Particulate–Polymer Composites. *Compos. Part B-Eng.* **2008**, *39*, 933-961.
(57) Bai, Y.; Ma, C.; Wang, P.; Fan, Z.; Bai, W.; Xiong, C.; Tang, C. Effect of Particle Size and Surface Modification on Mechanical Properties of Poly(Paradioxanone)/Inorganic Particles. *Polymer Composite.* **2012**, *33*, 1700-1706.
(58) Li, H.; Wang, R.; Hu, H.; Liu, W. Surface modification of self-healing poly(urea-formaldehyde) microcapsules using silane-coupling agent. *Appl. Surf. Sci.* **2008**, *255*, 1894-1900.
(59) Zhao, X.; Li, L.; Li, B.; Zhang, J.; Wang, A. Durable Superhydrophobic/Superoleophilic PDMS Sponges and Their Applications in Selective Oil Absorption and in Plugging Oil Leakages. *J. Mater. Chem. A* **2014**, *2*, 18281-18287.
(60) Rinaldi, A.; Tamburrano, A.; Fortunato, M.; Sarto, M. A Flexible and Highly Sensitive Pressure Sensor Based on a PDMS Foam Coated with Graphene Nanoplatelets. *Sensors* **2016**, *16*, 2148:1-18.

(61) Patel, P. S.; Shepherd, D. E.; Hukins, D. W. Compressive Properties of Commercially Available Polyurethane Foams as Mechanical Models for Osteoporotic Human Cancellous Bone. *BMC Musculoskelet. Disord.* **2008**, *9*, 137.
(62) Nichols, W. W. Clinical Measurement of Arterial Stiffness Obtained from Noninvasive Pressure Waveforms. *Am. J. Hypertens.* **2005**, *18*, 3-10.
(63) Munir, S.; Jiang, B.; Guilcher, A.; Brett, S.; Redwood, S.; Marber, M.; Chowienczyk, P. Exercise Reduces Arterial Pressure Augmentation through Vasodilation of Muscular Arteries in Humans. *Am. J. Physiol. Heart Circ. Physiol.* **2008**, *294*, H1645- H1650.
(64) Li, F. F.; Wang, Y.; Sun R.; Xue, S.; Yao D.; Shen, H. D.; Pulse Wave Analysis in Patients with Coronary Heart Disease Based on Hilbert-Huang Transformation and Time-domain. *Chin. J. of Biomed. Eng.* **2013**, *22*, 47-54.

GRAPHICAL ABSTRACT